Positioning and Control of an AUV inside a water pipeline for non-contact in-service Inspection

Unnikrishnan V. Painumgal*, Blair Thornton*, Tamaki Ura†, and Yoshiaki Nose*
*Institute of Industrial Science, The University of Tokyo, Japan
Email: unni, blair, nose@iis.u-tokyo.ac.jp
† Center for Socio-Robotic Synthesis
Kyushu Institute of Technology, Japan
Email: ura@lsse.kyutech.ac.jp

***Abstract*—Water pipelines are an important part of our social infrastructure. Early failure detection of the pipelines will help to prevent breakdown and avoid the large cost involved if a accident occurs. As pipelines are enclosed environments and difficult to access, pipeline inspection robots are increasingly used for routine inspection and early failure detection. In our research we propose the use of a small untethered AUV for the visual inspection of the pipeline interior. The vehicle carries optical sensors to aid non-contact motion inside the pipeline and also to capture images of the pipeline interior. The vehicle has identical front and rear sections and has a pair of cone laser and fish eye camera on either ends. The cone lasers and cameras act as range sensors as well as payload to capture pipe line interior images. A realtime vision based control system was developed for the autonomous operation of the proposed vehicle inside pipelines. A new offline position estimation algorithm estimates lateral position and pose of the vehicle inside pipeline. Laboratory experiments were performed in a test pipeline without and with water flow. The results of the experiment show that the proposed technique is efficient for non-contact inspection of a pipeline and helps to make vehicle compact to navigate through the enclosed environment inside pipelines.**

***Index Terms*—Cone laser, Vision based control, Navigation, AUV, Pipeline inspection**

I. Introduction

Water pipelines play a vital role in our everyday life. They can be found in homes, offices, industries, public facilities like railways stations, airports, schools and universities etc. A severe breakdown of a pipeline can lead to large costs and also lead to pollution and accidents. Hence routine inspection and maintenance of the pipelines is necessary for their trouble free performance. Water supply is a basic public service and therefore inspection tasks cannot compromise on the continuity or quality. An inspection system should be capable of operating when the pipeline is in-service. Since the quality of the water cannot be compromised, it is necessary that the motion should not be abrasive to avoid contaminating the clean water with particles chipped off from the pipe walls. Today several different pipeline inspection robots exist [1]–[7]. The pipeline inspection robots presently available use the contact with the walls for motion and also to position the robot to the centre of the pipe [8]. This may contaminate the water in old pipelines due to debris produced from corroded surfaces.

This paper proposes a new technique for non-contact positioning and control of an AUV for in-service inspection of water pipelines. The aim for developing this inspection system is to enable non-destructive and non-disruptive inspection of water pipelines. The basic constrains considered during the development of the system is to keep the system simple and multifunctional, so that the AUV platform can be made smaller and compact in size.The system will aid as a tool for routine preventive maintenance of pipelines and reduce large costs associated with potential failures [9]. We first describe the problem and challenges in developing a compact position sensing system for a pipeline inspection AUV. Then a newly developed conceptual AUV named PICTAN with the proposed positioning and control system is described. The innovative features incorporated in the vehicle for size reduction is also presented. A realtime vision based control system developed for non-contact position sensing and control is explained in detail. A vision based algorithm developed to estimate the lateral position and orientation of the vehicle in the pipeline is also presented. Laboratory experiments to verify the performance of the proposed system is also presented and the results are discussed.

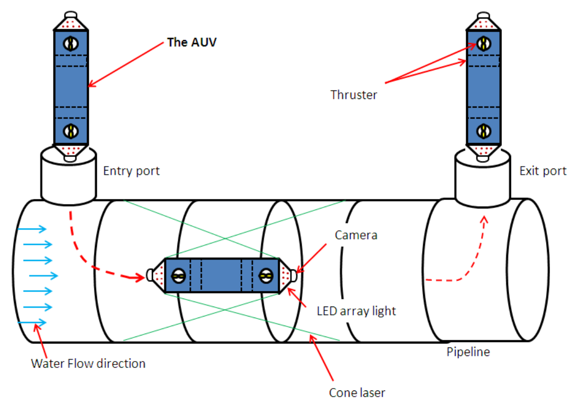

Fig. 1. Schematic of proposed Pipeline Inspection System

II. Problem Description and Solution

Water pipeline networks experience continues growth and therefore contains sections of new to moderately old and very old pipelines. Hence it is important for the pipeline internal inspection system to be able to enter and leave pipeline with

978-0-933957-40-4 ©2013 MTS

least disruption or damage to the existing pipe. This can be achieved only if the pipe inspection system can enter the pipeline through standard inspection ports or division valves which are several times smaller than the diameter of the main pipeline [10]. Large pipeline network means length of pipeline network to be inspected in large. Hence autonomous and tether free operation will be ideal for long distance inspection and to avoid cable entanglement. Therefore Autonomous Underwater Vehicles (AUVs) are ideal tools for pipeline internal inspection. However present AUVs are primarily designed for operation in the open ocean. Their navigation sensors are large in size and need high power for operation. Acoustic sensors like Doppler Velocity Log (DVL) and Sonar range sensors cannot be used inside pipelines due to large reverberations that can occur in such enclosed environment. The earth's magnetic field gets shielded inside metal pipelines. Hence magnetic compass based navigation sensors cannot be used inside pipelines. Recently torpedo shaped ocean going AUVs [11], [12] have been modified for inspecting large pipelines. The vehicles have been used to inspect very large pipelines with more than 2 meter diameter. Torpedo shaped AUVs also need large diameter chambers which are several meters in diameter for launch and retrieval. Hence it will difficult to use these vehicle in smaller distribution mains pipeline which are less than 1 meter in diameter and have inspection ports of 100mm to 150mm in diameter [13]. Considering the above facts a small AUV named PICTAN was developed which has specially designed multifunctional sensing capabilities for aiding autonomous motion inside pipelines and the small size enables it to enter and exit through small inspection ports. An illustration of the proposed pipeline inspection system is shown in figure 1.

III. PICTAN THE PIPELINE INSPECTION AUV

PICTAN is a small conceptual AUV which is primarily developed for conducting visual inspection inside fully flooded water pipelines. PICTAN stands for Pipeline Internal Condition Tansa. Tansa means inspection in Japanese. The vehicle is 675mm long and 108mm in diameter and can be inserted in to pipelines with inner diameter 700mm or larger. The vehicle is cylindrical in shape and it has a small diameter, hence it can enter and exit the pipeline through standard inspection ports. Water pipelines inherently has a flow inside it and the velocity of flow can vary based on the size of the pipeline and its designed capacity. The vehicle is near neutrally buoyant and it takes advantage of the flow inside the pipeline to move forward along with the flow. This eliminates the need for a thruster for forward motion and in turn reduces the energy requirement. The vehicle draws power from its on-board Lithium-ion battery and hence with reduced power consumption the vehicle can inspect long distances. The vehicles front and rear sides are identical and it has a set of green cone laser, fisheye lens camera and LED array lights on both ends. The Laser, Camera and Lights act as a multifunctional optical sensor system. Pipeline interior environment is dark and so the lights and camera is used for capturing illuminated images of the pipeline interior. The cone lasers are used for estimating the position of either end of the vehicle. The vehicle has four flushed in tunnel thrusters used for position control. The tunnel thruster gives a purely cylindrical profile to the body of the vehicle and aids smoother entry and exit from the pipelines through circular ports. The cone laser and the thrusters form part of a closed looped control system to guide the vehicle through the centre of the pipe and prevent hitting the walls of the pipe. The images captured by the two cameras are recorded in the onboard SD memory of the vehicle. After the survey the images can be downloaded using a tether cable and processed in off-line to extract valuable information about the interior condition of the pipeline being inspected. Two PX270 based micro-controllers in the vehicle handles the image processing tasks and operates the thrusters to perform autonomous position control of the vehicle. The table I gives the specification the AUV PICTAN. The figure 2 shows a photograph of the actual developed vehicle.

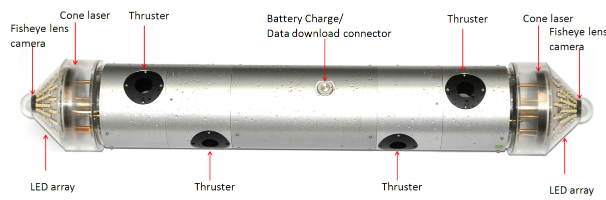

Fig. 2. PICTAN, Pipeline Inspection AUV

TABLE I
SPECIFICATIONS OF PICTAN

Specification	
Size	Length 675mm Diameter 108mm
Mass	4.8kg
Optics	Fisheye Camera×2 Cone Laser: 532nm 30mW×2 Light: 162 LED array×2 Luminous flux: 915 lm each
Thrusters	0.22N×4
CPU	PXA 270 520MHz×2
Battery & Duration	14.8V, 5200mAh Li-ion, 4hrs
Target Pipe Size	ø 700mm to 1200mm
Minimum entry/retrieval port size	ø110mm
Maximum operating pressure	150kPa

IV. OPTICAL SENSING SYSTEM

The camera and the cone laser source together act as a Optical Position Sensing System. The two sensing systems one in the front and one in the rear are identical in functionality and estimates the position of the front and the rear section of the vehicle respectively. A schematic of the Cone laser Camera sensing system is shown in figure 3. The schematic is a simplified two dimensional view of the sensor conditioning the vertical sectional plane passing through the principle axis of the sensor. In the figure we can see that the principle axis of the camera and the principle axis of the cone laser are collinear. The sensor system is also mounted on the vehicle

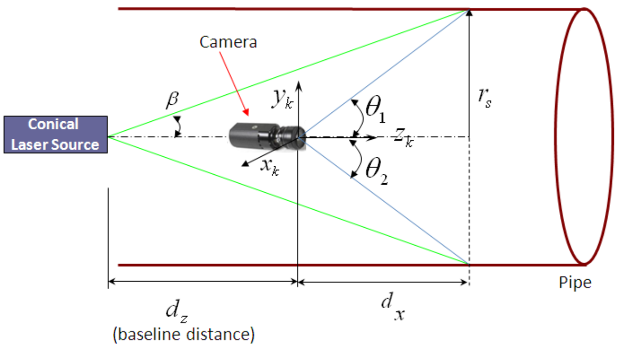

Fig. 3. Optical Sensor Schematic

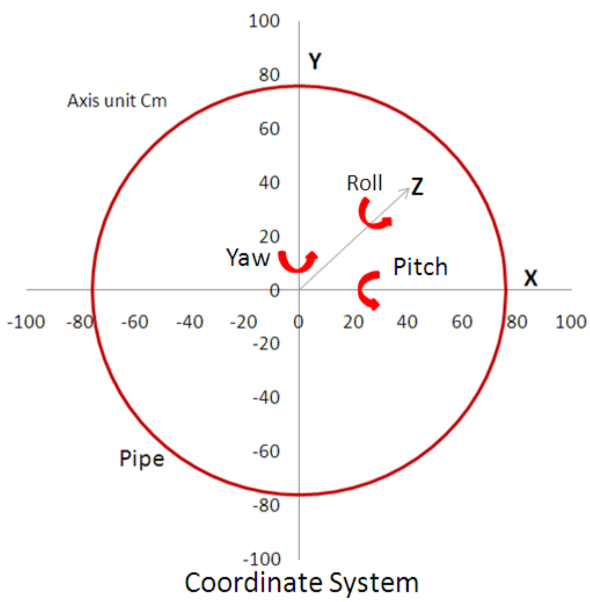

Fig. 4. Pipeline Coordinate System

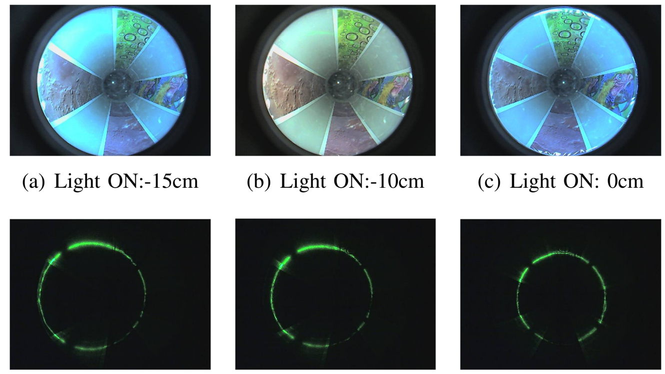

(a) Light ON:-15cm (b) Light ON:-10cm (c) Light ON: 0cm

(d) Light OFF:-15cm (e) Light OFF:-10cm (f) Light OFF: 0cm

Fig. 5. Images captured by vehicle when displaced and at centre

collinear to its hull principle axis. The camera and the cone laser are displaced by a distance called the baseline d_z. The angle β is the opening angle of the cone laser. The angle θ_1 and θ_2 are the angles that the reflected ray of light from the surface of the pipe wall makes with the principle axis of the camera. Assuming a constant pipe radius and cone laser angle angle β, the angle θ_1 and θ_2 vary based on the position of the vehicle. When the vehicle is perfectly aligned to the centre axis of the pipe the angles θ_1 and θ_2 are equal. When the vehicle moves towards the top of the pipe the angle θ_1 increases and the angle θ_2 decreases. When angle θ_1 increases the cone laser image captured by the camera will appear more closer towards the edge of the image frame in the top and cone laser image towards the bottom will appear more closer to the centre of the image frame.

In the actual sensor the light rays entering the camera from all 360 degrees around the optical axis of the camera will be affected by the position of the vehicle. When the vehicle is at the centre the theta angles all around the axis will be equal and so we will see a perfectly circular cone laser image, with centre coincident to the image frame centre. When the vehicle moves away from the centre the cone laser images appear more elliptical and displaced from the centre of the image frame. A series of images were captured by the vehicles onboard camera to illustrate this phenomenon and is shown in figure 5. The row images on the top were captured with LED light on and the bottom row of images were captured with the light off at the respective locations. We can see from figure 5(f) that the cone laser image appear as a circle and is centred to the image frame. When the vehicle is moved by -10cm to the left in the y axis (coordinate system as shown in figure 4), the theta angle towards the left side is more than the right side and so we see the cone laser image shifts towards the left and it appears less circular. When the vehicle is further moved away from the centre by -15cm, we can see that the cone laser image further enlarges and moves more to the left side as seen in figure 5(d). Thus it is clear that inspecting the shape of the cone laser image it is possible to estimate the position of the vehicle. The cone laser images are used for realtime vision based control as well as for offline position estimation. The realtime vision based control is used to control the position of the vehicle to prevent hitting the walls of the pipe. The offline position estimation is used to calculate precise position and attitude of the vehicle by means of triangulation. The position estimation is a computationally costly process and hence it is done in offline to enable the vehicles onboard microcontroller to do the realtime position control at a high speed. This Offline position estimation strategy also enables using compact low powered microcontrollers on the vehicle.

V. Realtime Vision Based Control

In a related research work by the authors [14], a similar conical laser and camera is used to estimate position of a pipeline inspection AUV by shape signature matching technique. The system was slow and not suitable for realtime position estimation due to the inherent time consumed in looking up the image feature database and the shape matching process. The new simplified technique proposed in this section does not require large feature database files which needs larger memory and computational requirements. Feature data base generation and Camera calibration is also not necessary for the operation of the new sensor.

The PICTAN AUV has four thrusters to control its lateral position inside the pipe and keep the vehicle towards the centre of the pipe. Two thrusters mounted in the vertical plane are used to control the heave and pitch motion. Another two thrusters mounted in the horizontal plane are used to control the sway and yaw motion of the vehicle. The front section consists of one vertical and one horizontal thruster as shown in figure 2. The rear section contains another pair of thrusters. The optical sensor system in the front side is responsible for the control of the front side vertical and horizontal thrusters. Similarly the optical sensor system in the rear side is responsible for the control of the thrusters in the rear side. The front side and rear side realtime control is managed by separate microcontrollers. Microcontrollers have limited memory and processing ability and so to achieve realtime control a minimal computation load strategy is followed. Firstly during image capturing the vehicle is programmed to switch off its bright LED light in the front and rear in a time synchronised way. Once LED light is switched off a high contrast cone laser image is captured. This images appears as a green circle on a dark black background. The cone laser is represented by the brightest pixels in the image frame and hence it can be easily identified by the pixel search program shown in figure 6. To reduce the computational load further, only four points on the cone laser image are used for the realtime control. The top and bottom pixels location is used to control the vertical thruster and the left, right cone laser pixel location is used to control the horizontal thruster on one end of the vehicle. The cone laser image obtained by the camera on the rear side is used to control the rear vertical and rear horizontal thruster in the same manner. Thus by means of reducing the computational load it is possible to do realtime image processing at a rate of 10 frames/second.

A PID controller is used to control the thrusters based on the shape of the cone laser image. The control law is given in equation 1 and 2.

$$F_{fV} = K_p(p_{ft} - p_{fb}) + K_i \int (p_{ft} - p_{fb})dt + K_d(\dot{p_{ft}} - \dot{p_{fb}}) \quad (1)$$

$$F_{fL} = K_p(p_{fr} - p_{fl}) + K_i \int (p_{fr} - p_{fl})dt + K_d(\dot{p_{fr}} - \dot{p_{fl}}) \quad (2)$$

Here F_{fV} and F_{fL} are the force control commands for the front vertical thruster and front lateral thruster respectively. p_{fr}, p_{fl}, p_{ft} and p_{fb} are pixel locations of left, right, top and bottom points of the cone laser image as shown in figure 7. A similar control equation is applied based on the rear camera cone laser image pixel location to control the vertical and lateral thruster of the rear side.

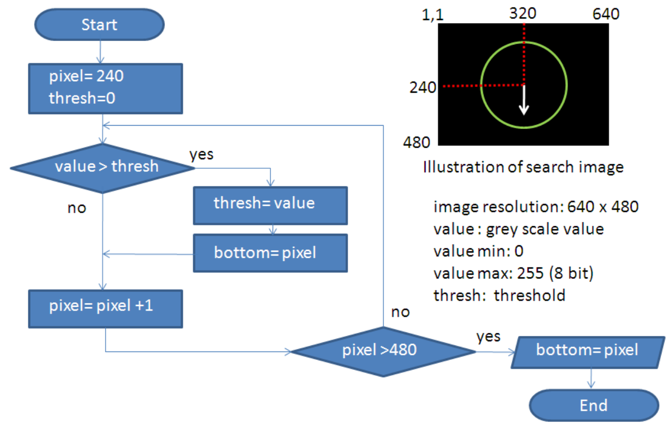

Fig. 6. Flowchart of pixel search program

VI. Offline Position Estimation Algorithm

The realtime control system explained in the previous section uses the deviation of cone laser shape from the perfect circular shape (when at pipe centre) to control the vehicle in realtime. The precise vehicle position is not calculated. However knowing the position and pose of the vehicle is important to estimate the size and extent of pipeline interior faults that may appear on the images captured by the vehicle. Vehicle position estimate can also be used to generate photo mosaics using a software described in [15].
Offline data analysis takes advantage of the high computational capability of desktop computer to implement complex algorithms. The offline position estimation algorithm analyses the cone laser images from the front and the rear camera to estimate the precise position and attitude of the vehicle in the pipeline coordinate system. The centre of the pipe is the origin of the coordinate system as shown in figure 4.

A block diagram of the steps involved in the position estimation process is shown in figure 7. The cone laser images recorded by the vehicle during motion inside the pipe is downloaded from the vehicles memory and is used as input to the position estimation algorithm. It should be noted that the front and rear end camera of the vehicle are time synchronised and indexed. The front and rear camera image at one instant of time acts as input to the algorithm. The algorithm uses pixel location of four points on a cone laser image namely top, bottom, left and right as shown in the figure. Together with front and rear camera images, a total of 8 cone laser points are used for the whole position estimation process. The pixel search program descried in figure 6 is used to search the points on the cone laser. The vehicle has a AHRS compass device mounted internally and the roll angle is recorded for every image captured. This vehicle roll angle is used to compensate for vehicle roll during the pixel search process. Next the slant radial distance of the vehicle is calculated for both the front and rear image. The slant radial distance is the distance between the principle axis of the optical sensor and the wall of the pipe represented by r_s in figure 3. This distance equals to the radius of the pipe when the vehicle is perfectly aligned

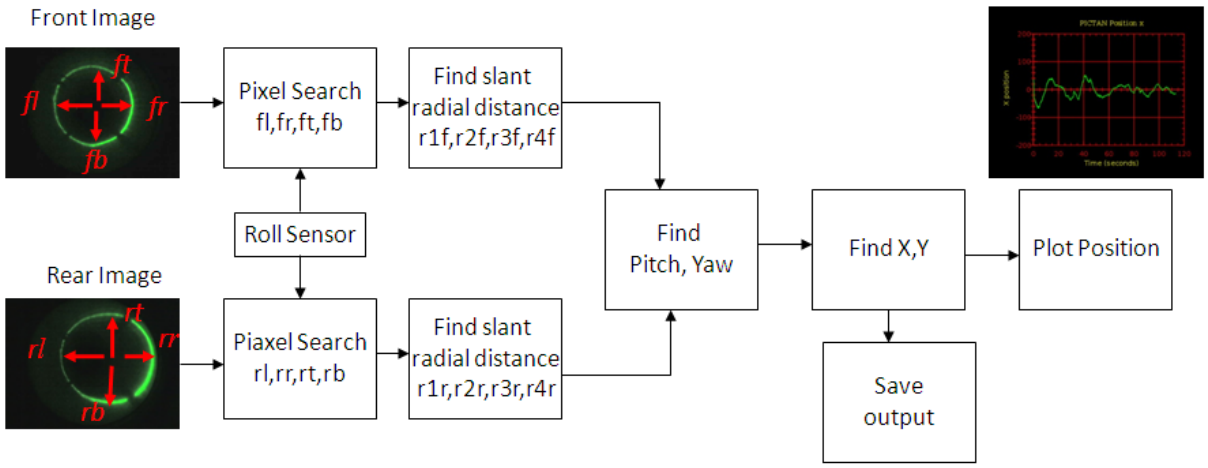

Fig. 7. Offline position estimation process

to the centre of the pipe. In this case the top, bottom, left and right slant radial distances are equal to the radius of the pipe. However when the vehicle experiences linear or angular displacement the four slant radial distances tend to be different from each other and can be larger or smaller than the radius of the pipe. Combined together the four slant radial distance contain the position information of one end of the vehicle. For each cone laser point one slant radial distance is calculated and so 8 slant radial distance is calculated. The equation for calculating slant radial distance is given by equation 3.

$$r_s = d_z \left(\frac{sin\theta sin\beta}{sin\theta - sin\beta} \right) \tag{3}$$

The inputs to the above equation are angle β, θ and baseline distance d_z. The angle β and distance d_z are known values and exact values can be obtained from the CAD design of the vehicle. The angle θ is a camera dependent function which was calculated by camera calibration. A check board like pattern was used to do the camera calibration and a lens distortion curve was plotted. Through curve fitting a 6th degree polynomial equation (refer equation 4) was formed based on the experimental values.

$$\theta = 28.0x^6 - 113.3x^5 + 174.5x^4 - 124.2x^3 + 42.0x^2 + 45.3x + 0.1 \tag{4}$$

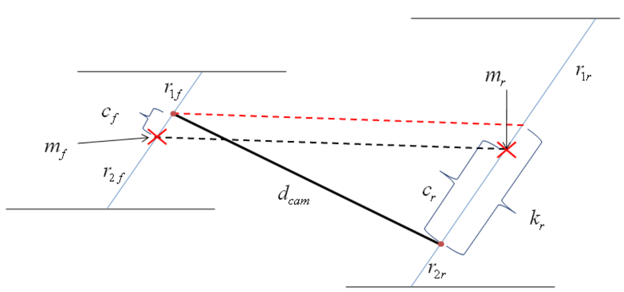

Fig. 8. Simplified side view of vehicle in pipeline

After the slant distanced for the front and rear side sensor is estimated, this value is used to calculate the angular displacement of the vehicle namely Pitch and Yaw. A simplified skeleton of the vehicle in the pipe viewed from the side parallel to the axis of the vehicle is illustrated in figure 8. In the figure the top and bottom slant radius of the front and rear camera is represented. Assuming that the pipe is perfectly circular in shape, the top and the bottom portion of the pipe where the laser strikes the pipe surface will be parallel to each other as seen in the figure. d_{cam} is the distance between the front and the rear cameras of the vehicle. In the image shown in figure 8 the distance k_r can be estimated from the four slant distance values r_{1f}, r_{2f}, r_{1r} and r_{2r}. The pich angle can be calculated using equation 5.

$$\theta_{pitch} = tan^{-1} \left(\frac{k_r}{d_{cam}} \right) \tag{5}$$

In a similar manner by using the four horizontal plane slant radius values, the yaw angle of the vehicle θ_{yaw} can be calculated. The pitch and yaw angle estimates can be used to find the lateral displacement of the vehicle from the sides of the pipe. The formulae for calculation the eight radial distance values of the front and rear section is given by the equations below.

$$R_{1f} = r_{1f} cos(\theta_{pitch}) \tag{6}$$

$$R_{2f} = r_{2f} cos(\theta_{pitch}) \tag{7}$$

$$R_{3f} = r_{3f} cos(\theta_{yaw}) \tag{8}$$

$$R_{4f} = r_{4f} cos(\theta_{yaw}) \tag{9}$$

$$R_{1r} = r_{1r} cos(\theta_{pitch}) \tag{10}$$

$$R_{2r} = r_{2r} cos(\theta_{pitch}) \quad (11)$$

$$R_{3r} = r_{3r} cos(\theta_{yaw}) \quad (12)$$

$$R_{4r} = r_{4r} cos(\theta_{yaw}) \quad (13)$$

A translational coordinate transformation is applied to the radial distance values to represent the position in of the vehicle front and rear side in the pipe centred coordinates. The position of the front (x_f, y_f) and the rear side (x_r, y_r) of the vehicle is used find the position of the centre point of the vehicle.

$$x = x_f + \left(\frac{x_r - x_f}{2}\right) \quad (14)$$

$$y = y_f + \left(\frac{(y_r - y_f)}{2}\right) \quad (15)$$

The equation 14 and 15 gives the position of the vehicle in pipeline centred coordinates.

A. Error estimation

The performance of the offline position estimation algorithm was evaluated by capturing ground-truth cone laser images with know X,Y, Pitch and Yaw values. The figure 9 shows the setup used to capture the ground-truth cone laser images. The images were captured in dry laboratory condition. A large 760mm diameter polyethylene pipeline is placed on a flat surface. The pipeline is formed by joining two 1.5meter long pipe sections. The two sections are axially aligned and joined firmly using four 0.4m long aluminium frames. The vehicle is placed inside the pipeline through the gap between the two section of pipe. The vehicle is placed on a pre-calibrated linear motion table which is aligned to the centre of the pipe. The vehicle can be given known linear displacements by rotating a mechanical handle on the linear motion table. Yaw angle can be simulated by using a rotary stage on the setup. The heave position of the vehicle can be raised or lowered by using height adjustment screw. Pitch angle was introduced by using a wooden plank of known height.

Ground truth images were captured with various form of displacement of the vehicle evenly distributed over the designed range of the position sensor. The obtained cone laser images were indexed with their respective ground truth position data manually noted from the experiment setup. The ground truth images were input to the position estimation algorithm. The position estimate was compared to ground truth data to evaluate the accuracy and error produced by the algorithm. The figure 10 shows a position estimate plot generated by the algorithm for a set of ground truth images. In this set of data the vehicle was induced a Yaw angle displacement of 10°, the Pitch angle is zero and Y displacement (vertical) is also zero. The vehicle is placed 70mm horizontally displaced (X=70mm) from the centre of the pipe and moved towards the left up to X=-100mm. The vehicle is moved horizontally

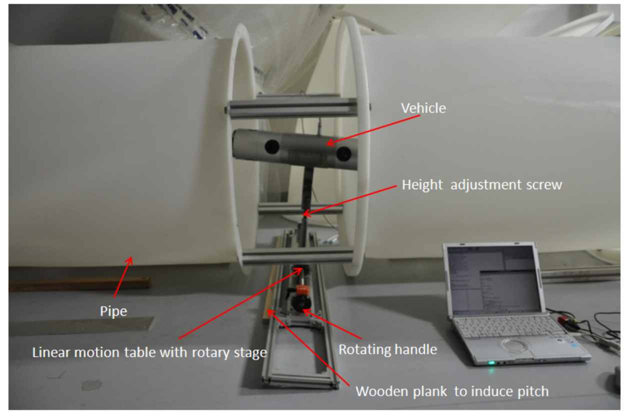

Fig. 9. Ground truth image capturing setup

by rotating the handle on the linear motion table. Images were taken at every 10mm interval. The figure 10 contains four plot windows. Each plot window contain the position estimate for an individual degree of freedom. The plot on the top left shows the X position and the one on top right shows Y position. The plot in the bottom left and right represent the Pitch and Yaw estimates of the vehicle. The X and Y position is represented in mm and Pitch, Yaw estimates are represented in degrees. The y axis in all the plot labelled as data serial number represent the order in which the ground truth images were captured. In this case from X=70mm to X=-100mm. In this dataset the Y, Pitch and Yaw values are constant values and the X value is the variable quantity. We can see from the plot represented by green star marker, that the position estimates are every close to the ground truth values. The error in the position estimate increases when the cone laser image is formed closer to the edge of the image frame where lens radial distortion is high. This error can be reduced by using accurately pre-calibrated camera lens. The error of the position estimates using a large set of ground truth data was calculated. The error was calculated using the function given in equation 16.

$$\% \, error = \frac{\sqrt{(v_{actual} - v_{measured})^2}}{range} \times 100 \quad (16)$$

The specification sheet formed based on the design of the sensor and the ground-truth experiment is given in table II.

TABLE II
SPECIFICATIONS OF POSITION ESTIMATION SENSOR

Feature	Value
Reference pipe diameter	$\phi 760mm$
X range	-130mm to +130mm
Y range	-130mm to +130mm
Pitch range	-10° to +10°
Yaw range	-10° to +10°
X,Y position error max.	5.7% of range
Pitch,Yaw error max.	11.5% of range

VII. Experiments and Results

Experiments were conducted in laboratory conditions to verify the performance of the realtime vision based control

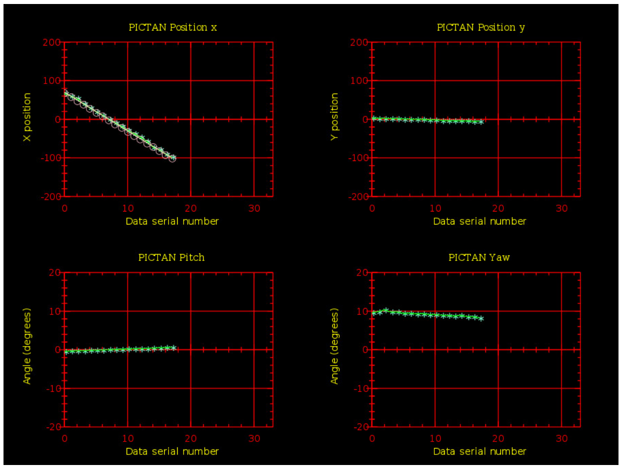

Fig. 10. Position estimate for Ground truth value: X=70 to -100 Y=0 Pitch=0 Yaw=10 degrees

system and the offline position estimation algorithm was used as a tool to estimate the path followed by the vehicle during the experiment. The experiments conducted can be divided in to two types. One experiment was conducted in a water flooded pipline with still water and another experiment was conducted in a pipeline with a constant water flow.

A. *Experiment in still water pipeline*

The figure 11 shows the experimental setup for the still water pipeline experiment. A fresh water tank of 7m Length×7m Breadth× and 7m Depth was used for the experiment. The same polyethylene pipe used for the ground truth image capture was used. The pipeline has a window of 400mm in the middle through which the vehicle can be launch and retrieved. The water is perfectly stand-still and so no external disturbances like waves or flow is affecting the vehicle in these experiments. A magnetic switch is triggered using a magnetic pole to turn on the vehicles control system during the experiment. The vehicle buoyancy is trimmed to achieve near neutral buoyancy. The vehicle is positively buoyant by <8 grams to prevent the vehicle from sinking to the floor of the 7m deep tank.

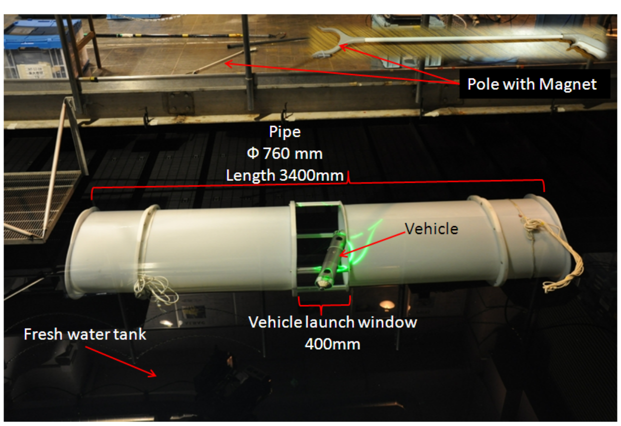

Fig. 11. Experiment setup for still water experiment

In this test the vehicle was placed at the top extreme of the pipe touching the top side of the pipe due to its positive buoyancy. The figure 12 shows the various stages in the experiment illustrated through video frames captured at the respective time stamps printed on each of the video frame. At time 00:14 we see that the vehicle is placed at the top of the pipe. The cone laser appear at a narrow diagonal angle which implies that the vehicle is touching the top of the pipe. At time 00:15 the vehicle is switched on with the magnetic pole, so we see the LED flashing. After switch on, the pole is immediately removed and a delay count down timer goes on in the vehicle until 00:28 to start the control system. Once control system is started both the vertical thrusters are automatically powered by the control system and the vehicle starts diving towards the centre of the pipe. By time 00:47 the vehicle reaches the centre of the pipe and we see circular laser images at both sides of the vehicle as shown in the image.

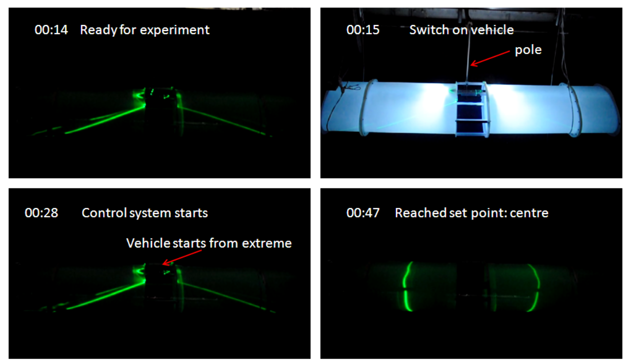

Fig. 12. Different stages during the still water experiment

A position estimate from the experiments cone laser image data is shown in figure 13. In the graph we see that up to 15 seconds the Y position and the pitch position data has noise due to the clipping of the laser image. After that from Y=100mm we see that vehicle swiftly descends down and settles down near the centre of the pipe. The pipes radius is

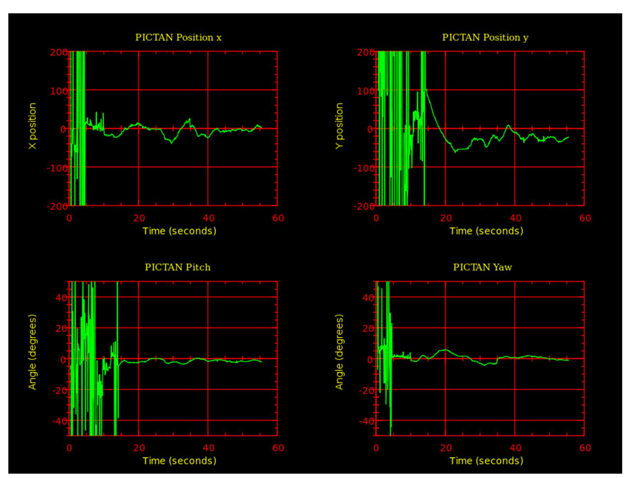

Fig. 13. Position estimate for the still water experiment

380mm and the vehicles radius is 50mm. Hence the vehicle has dived a total of 330mm to reach the centre of the pipe in 19 seconds as seen from the video frame and the position data. The vehicle experiences minimal pitch and yaw movements during this test. The X position oscillates around 30mm and stabilizes to centre of pipe after 40 seconds. Thus the experiment demonstrates the capability of the realtime vision based control system to autonomously position the vehicle to the centre of the pipeline from extreme positions. This will prevent the vehicle from hitting the walls of the pipeline during actual inspection.

B. Experiment in pipeline with flow

The autonomous control experiment described in the previous section was conducted in still water. However the target application of the vehicle is to inspect in-service pipeline with flow. Therefore a realtime autonomous control experiment was conducted on the vehicle by simulating flow in a section of pipeline. The experiments with simulated flow was conducted at the water channel experimental facility of the Public Works Research Institute(PWRI) at Tsukuba. The Water channel is 1.0m wide, 1.3m tall and 15m long. Water is supplied in to the channel using an electric pump with a maximum capacity of 280L/s. The pumping capacity is variable. The height of water in the channel and flow rate can be varied by varying the pumping capacity.

A photograph of the experiment setup is shown in figure 14. The pipeline used for the experiment was 4400mm long including a 400mm launch window. The water level was set to 890mm so that the pipe is fully immersed in water . To prevent the pipe from moving due to force induced by flow, it is attached firmly to the walls of the water channel by using aluminium frames as seen in the figure. The vehicle is launched at one end of the pipe and retrieved at the other end by using safety nets. An electromagnetic flow sensor was used to measure the flow inside the pipe during the experiments. A mean flow rate of 30mm/s was maintained during the experiment.

An underwater video camera was placed at the exit end of the pipe to document the experiment. The figure 15 shows

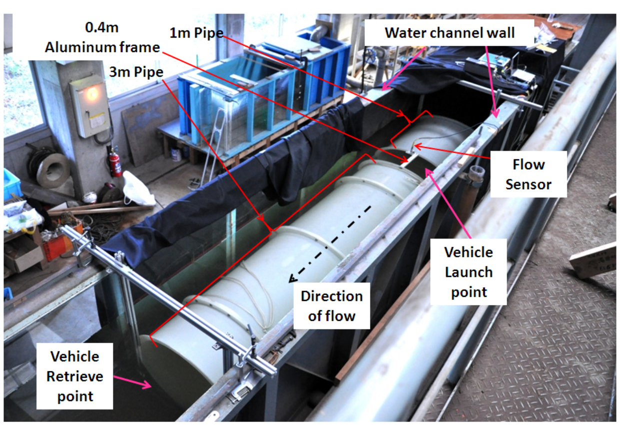

Fig. 14. Flow test experiment setup

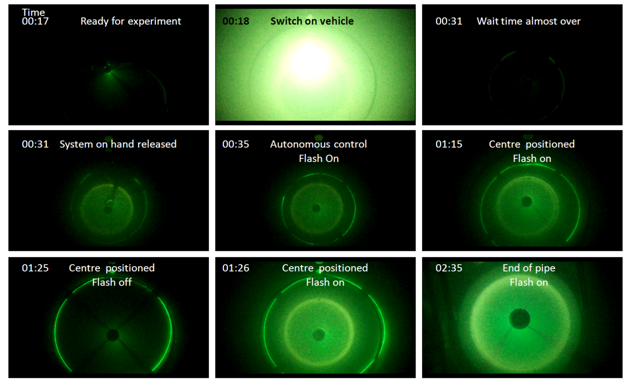

Fig. 15. Video frames from the multitasking test with control

the video frames captured during this experiment. During this experiment the vehicles rear LED array light flashed every 2 seconds and captures illuminated data apart from the standard cone laser images with dark background. The front light was not flashed to prevent saturated images in the video. In the video frame 00:17 the vehicle is launched in to the pipe and is ready for the test. At 00:18 the vehicle is switched on using the magnetic pole. The vehicle blinks its LED lights to indicate switch on. The image appears saturated with green color because the underwater camera capturing this video is looking straight towards the green cone laser of the vehicle. Then the vehicle waits 15 seconds before automatically switching on the control system. At 00:35 the vehicle control system is ON, indicated by the first light flash as seen in the image. Until this time the vehicle was held at the centre of the pipe by hand and now the vehicle is released to move freely with the flow in the pipe until it reaches the end of the pipe. After control system is switched on the vehicle actively uses all its four thrusters to enable position keeping at the centre of the pipe.

In this experiment the flashing LED lamp periodically illuminates the pipeline interior, which is captured by the vehicles camera. While illuminated images are important as a payload for the vehicle, it can cause trouble to the control system due to poor visibility of cone laser. Internally in the control system a new thresholding based image processing program was used to eliminate the illuminated images from the control loop calculation and instead uses the cone laser data from previous image. In the figure 15 we see that from the 4th frame at 00:35 the vehicles control system maintains the position of the vehicle in the centre of the pipe until the vehicle exits the pipe which is seen in frame 02:35. In frame 01:25 the flash is off. All the other frames were chosen on purpose to have flash light so that pipe interior is visible in the image. At 02:35 the image shows a larger pipe circumference because we are viewing the end flange of the pipe in this image, which is closer to the underwater camera used to capture this video.

A position estimate of the vehicle from the experiment image data is shown in figure 16. From the beginning of the test until 30 seconds we see that vehicles path is clearly

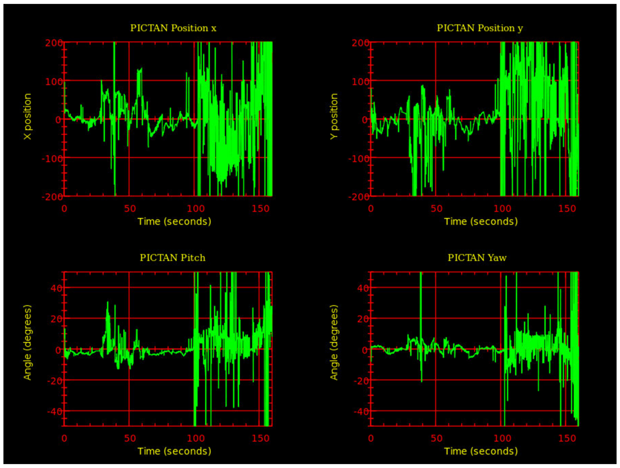

Fig. 16. Position data from the multitasking test with control

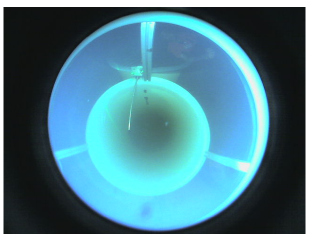

(a) Crossing launch window

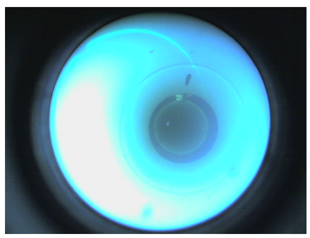

(b) 27 seconds later

Fig. 17. Illuminated images captured by vehicles onboard camera

estimated and the vehicle is close to the pipe centre. We see noise in the position estimate at the region where the vehicle crosses the launch window due to the occlusion of the cone laser. After 70 seconds until 100 seconds there is less noise in the position estimate and we can see that the vehicle maintains its position towards the centre of the pipe. Inspecting the underwater experiment video, we found that the vehicle was stable and controlled its position towards the centre of the pipe between the start and end of the experiment. However the position estimates are not clearly visible and filled with noise because of the short length of pipeline used for the experiment. The launch window and short length of pipeline used in the experiment setup caused the cone laser to fall outside the pipeline. Hence the cone laser in one end of the vehicle was not visible by the vehicles camera in many occasions during the experiment. It can be noted that the offline position estimation algorithm is capable of estimating the position of the vehicle only if both end cone lasers are clearly visible. This lead to the noisy position estimates in the flow test. However the vehicles front and rear control systems are independent. Hence even if only one cone laser is visible the two thruster in the respective end of the vehicle is controlled.

The figure 17 shows some of the illuminated images captured by the vehicles onboard fisheye camera. In the first picture we see that the vehicle is passing through the launch window. The metallic rod protruding into the centre of the pipe is the flow sensor. In the second picture which was captured 27 seconds after the previous picture, the vehicle has almost reached the end of the test pipeline and the launch window is visible at a far distance. The visibility in the images is poor due to the turbid water present in the experiment facility. From the images and the position data we see that the vehicle is capable of doing multitasking using the camera by doing realtime vision based control as well as image capturing, which is a necessary feature in the vehicle during actual pipeline inspection.

VIII. Summary and Conclusion

This paper proposes a novel technique for positioning and control of an AUV for pipeline internal inspection. The proposed system aids non-contact and non-destructive inspection of pipeline interior. The sensing system is used for control of the vehicle as well as payload to capture images of the pipe interior. The sensor multitasking enables reduced components in the vehicle and supports miniaturisation of the vehicle. The strategic reduction of computational load in the control system image processing steps aids using small and less power consuming microcontroller on-board the AUV. Results of the experiments conducted in the test pipeline shows that the vehicle is capable of autonomously inspecting pipelines while being tetherless. Experiments with simulated flow was conducted at a slower flow rate due shorter test-pipeline length. Short test pipe line was used due to the practical problems like limited length of water channel facility. In actual pipelines the vehicle is capable of operating at higher flow rates. To operate the vehicle in actual pipelines a launch and recovery system has to be developed. The launch and recovery system should be sealed and pressure compensated to prevent water leakage and interruption to the service during inspection. A launch and recovery system will be developed in future to demonstrate the operation of the AUV in actual pipelines. Data processing and reporting software is also an important area of future research.

Acknowledgements

The authors would like to express their sincere thanks to the director and staffs of PWRI, Tsukuba for extending their kind help to use their water channel facility to conduct the flow tests described in this paper.

References

[1] Majjid. M. Moghaddam, Alireza Hadi, *Control and Guidance of a Pipe Inspection Crawler (PIC)*, 22nd International Sysnposium on Automation and Robotic s in Construction, 2005.

[2] Harry T. Roman, Bruce A. Pellegrino, *Pipe Line Crawling Inspections: An Overview*, IEEE Transactions on Energy Conversion, Vol. 8, No. 3, 1993.

[3] K. Suzumori, K. Hori, T. Miyagawa, *A Direct Pneumatic Stepping Motor for Robots: Designs for Pipe inspection Microrobots and for Human Care Robots*, IEEE International Conference on Robotics and Automation, pp. 3047-3052, 1998.

[4] S. Hirose, H. Ohno, T. Mitsui, K. Suyama, *A Direct Pneumatic Stepping Motor for Robots: Design of Inpipe Inspection Vehicles for ϕ25,ϕ50,ϕ150 pipes*, IEEE International Conference on Robotics and Automation, pp. 2309-2314, 1999.

[5] M.Muramatsu, N. Namiki, R. Koyama, Y. Suga, *Autonomus Mobile Robot in Pipe for Piping Operations*, IEEE International Conference on Intelligent Robots and Systems, pp. 2166-2171, 2000.

[6] Roh, S.G.; Ryew, S.M.; Yang, J.H.; Choi, H.R., *Actively steerable in-pipe inspection robots for underground urban gas pipelines*, IEEE International Conference on Robotics and Automation, pp. 761 - 766 vol.1, 2001.

[7] Se-gon Roh, Hyouk Ryeol Choi, *Differential-drive in-pipe robot for moving inside urban gas pipelines*, IEEE Transactions on Robotics and Automation, Volume 21,Issue 1, pp. 1 - 17, 2005.

[8] Jun Okamoto, Julio C. Adamowskia, Marcos S.G. Tsuzukia, Fla vio Buiochia, Claudio S. Camerinib, *Autonomous system for oil pipelines inspection*, Mechatronics , Elsevier, pp. 731-743(13), 1999.

[9] Tokyo Water Works Waterworks Bureau, *Replacement Project of Aged Pipes in Tokyo*, IWA World Water Congress VIENNA, 2008.

[10] Tokyo Metropolitan Waterworks Bureau *Leakage Prevention Guidebook page: 1*, http://www.waterprofessionals.metro.tokyo.jp/kat.html., 2011.

[11] H.Najjaran, *IRC creating an underwater robotic vehicle to inspect in-service water mains*, Construction Innovation, vol. 10, no. 2, 2005.

[12] Jorg Kalwa, *SeaCat AUV Inspects Water Supply Tunnel*, Sea Technology Magazine http://www.sea-technology.com/features/2012/0812/seaCat.php, 2012.

[13] Tokyo Metropolitan Waterworks Bureau *Leakage prevention in Tokyo*, Tokyo Metropolitan Waterworks Bureau. http://www.waterprofessionals.metro.tokyo.jp/pdf/leakage_pervention_in_tokyo.pdf, 2008.

[14] P. Unnikrishnan, B. Thornton, T. Ura, and Y. Nose, "A conical laser light-sectioning method for navigation of autonomous underwater vehicles for internal inspection of pipelines," in *OCEANS 2009-EUROPE*. IEEE, 2009, pp. 1–9.

[15] Adrian Bodenmann , Blair Thornton, Tamaki Ura and Unnikrishnan V. Painumgal, *Visual Mapping of Internal Pipe Walls using Sparse Features for Application on board Autonomous Underwater Vehicles*, OCEANS 09 IEEE Bremen, Germany, 2009.